CHAPTER III

RESULTS AND DISCUSSION

3.1 The Characterization of Aminosilane Grafted onto the Silicate Clay

Powder samples of silicate and modified silicate clay were characterized by X-ray diffraction for the determination of crystal lattice spacing and for the grafting condition.

3.1.1 The XRD Characterization of Aminosilane Grafted onto the Silicate Clay

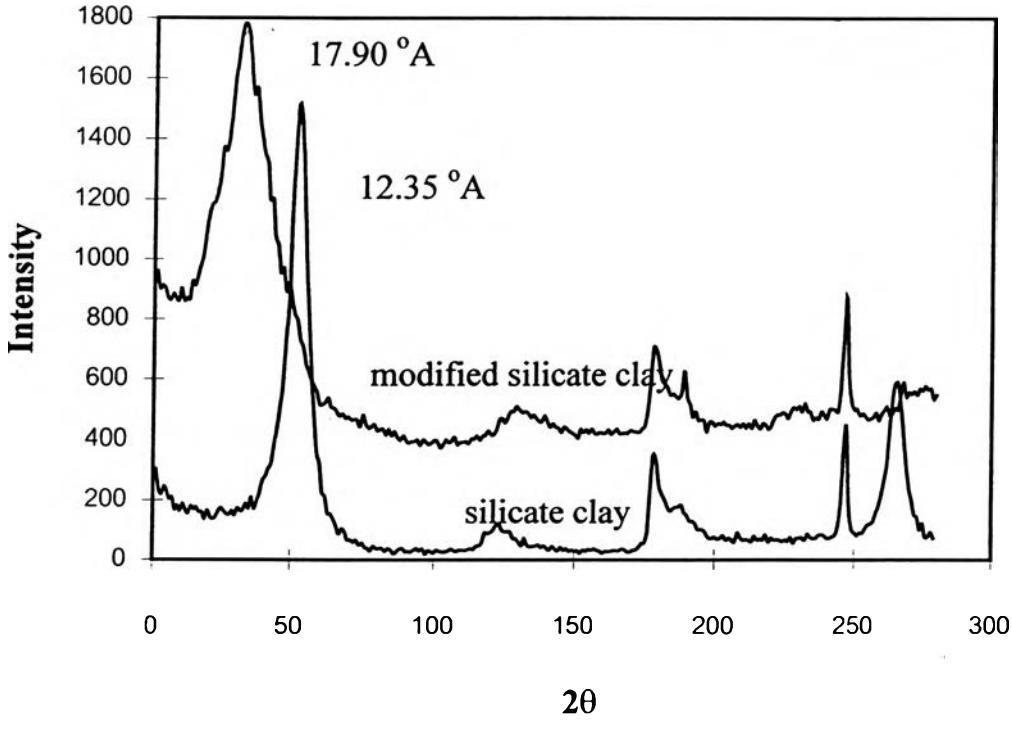

Figure 3.1 The X-ray diffractogram of silicate and modified silicate clay.

Figure 3.1 shows the X-ray diffractogram of the silicate clay and the modified silicate clay by the grafting of aminosilane to the silicate clay. The basal layer spacing was obtained from the (001) peak position. These peaks were assigned to the 001 lattice spacing of montmorillonite. The lattice spacing corresponds to an interlayer spacing of the silicate clay which was found to be 12.75 °A. For the modified silicate clay, it was 17.90 °A, showing the expansion of the interlayer space by 5.15 °A. This observation supported that the interlayer Na reacted through siloxane bond of the aminosilane used.

The expansion in the interlayer spacing can be depicted as shown in fig. 3.2

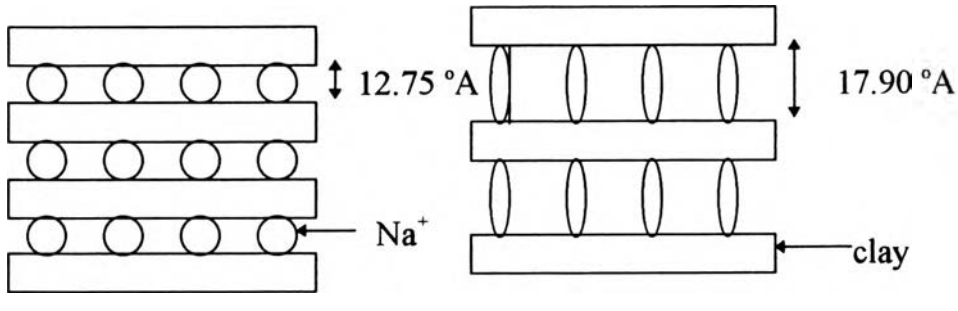

Na^+ type montmorillonite. Modified silicate clay

Figure 3.2 The intercalating behavior of montmorillonite.

The initial spacing of the Na+ Montmorilonite depends on the humidity and for the final spacing depends upon extent of intercalation and reaction. Jeon, Jung and Hudson [1995] prepared the Na^+- Montmorillonite by the intercalation with dodecylamine and found that the interlayer spacing peak shifted to a new value 16.5 °A from the old value of 11.8 °A belonging to the original clay.

3.1.2 Grafting Conditions

3.1.2.1 The influence of stirring time on the grafting condition

The experiments were done with 25 wt % aminosilane for finding the optimum stirring time for the deposit of aminosilane onto the silicate clay. By varying the stirring time between 10, 30, 60, 90 and 120 min. We found that all stirring times gave nearly the same result by the XRD characterization as shown in fig. 3.3. So the optimum stirring time chosen was 10 min.

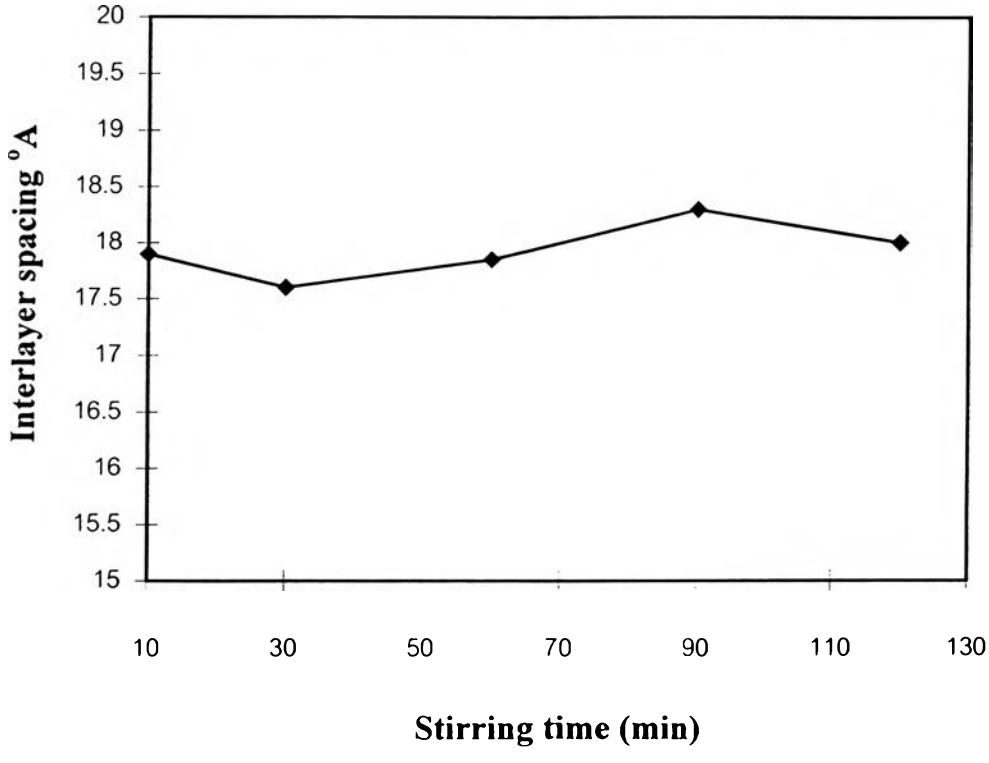

Figure 3.3 The influence of stirring time on the grafting condition.

3.1.2.2 The influence of drying time on the grafting condition

The effect of drying time on the grafting condition of aminosilane onto the silicate clay is shown in fig.3.4. The interlayer spacing determined by XRD is shown as a function of drying time. After a period of 48 hours of drying time we obtained the same value for the interlayer spacing. The silanol (SiOH) groups may first form hydrogen - bonds with the substrate surfaces, and during drying they condensed in to siloxane structures and perhaps chemically were bonded to the surface.

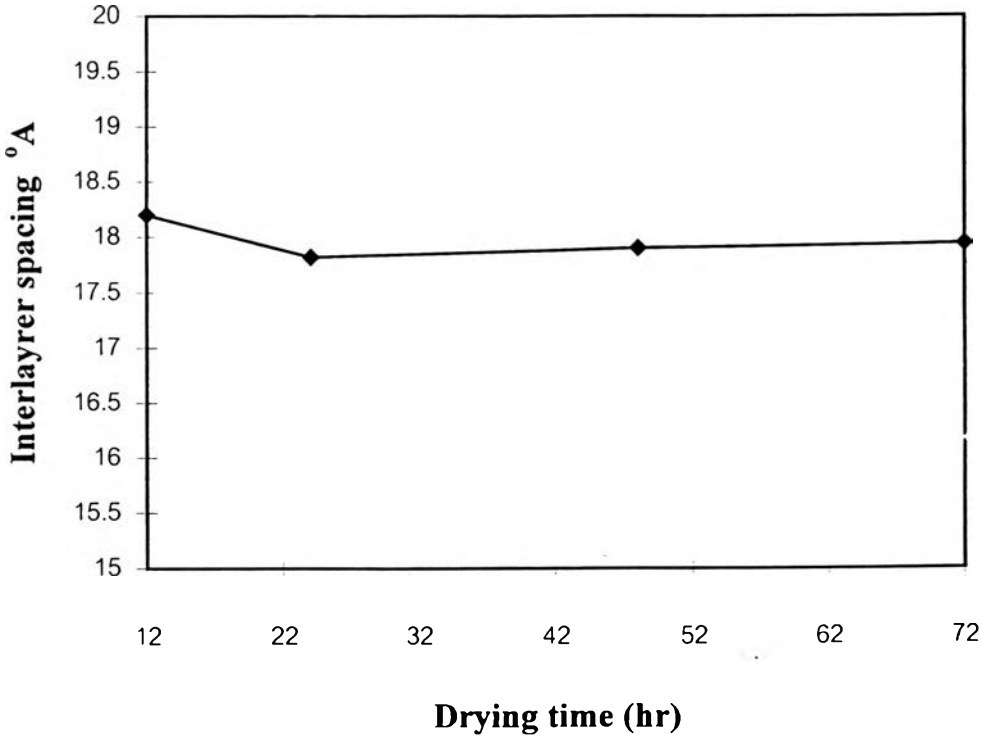

Figure 3.4 The influence of drying time on grafting condition.

3.1.2.3 The influence of silane concentration on interlayer spacing.

By using the XRD technique, we found that the basal spacing peak shift for the modified silicate clay, with 25 wt % aminosilane. For the percentage of aminosilane less than 15 wt %, the basal spacing peak shift could not be detected, perhaps because the aminosilane adopts a flattened conformation or because the aminosilane absorps or react first on the external surface of the particle. So the amount of 25 wt % aminosilane was chosen only to demonstrate the grafting condition.

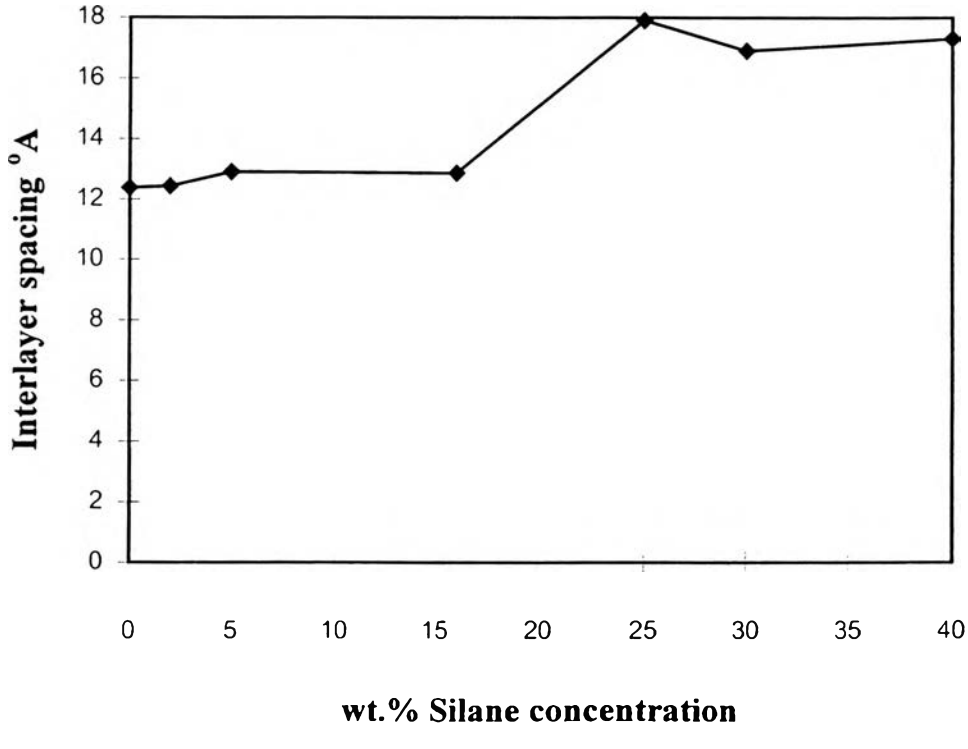

Figure 3.5 The influence of silane concentration on the grafting condition.

3.2 The Characterization of the Grafting MAPP to the Modified Silicate Clay

3.2.1 DRIFT Results

Similar model experiments using FTIR technique were used to demonstrate polymer chain grafting, i.e. the reaction between the silane coupling agent and MAPP. The experiments were carried out with 25 wt % aminosilane modified silicate clay and MAPP. Diffuse reflectance infrared spectroscopy (DRIFT) was used to obtain the IR spectra.

The lower spectrum in fig. 3.6 is that obtained from pure maleic anhydride modified polypropylene. The anhydride form appears as two peaks one at 1833 cm^{-1} and a larger one at 1782 cm^{-1}. The upper infrared absorbance spectra shown in fig. 3.6 are assigned to the MAPP grafted with is obtained after carrying out grafting onto modified silicate clay. The two peaks of the anhydride disappear, and new bands appear at 3300, 1663 and 1567 cm^{-1}. A very broad band appears at about 3300-3500 cm^{-1} due to the N-H stretching mode of amine. The two new bands at 1663 and 1567 cm^{-1} correspond to the amide group indicating that the aminosilane has reacted with the anhydride.

By using the reaction times of 30 and 60 min, we obtained the same spectra as shown in fig. 3.7. Thus reaction time of 30 min was chosen for the complete reaction between the MAPP and the modified silicate clay.

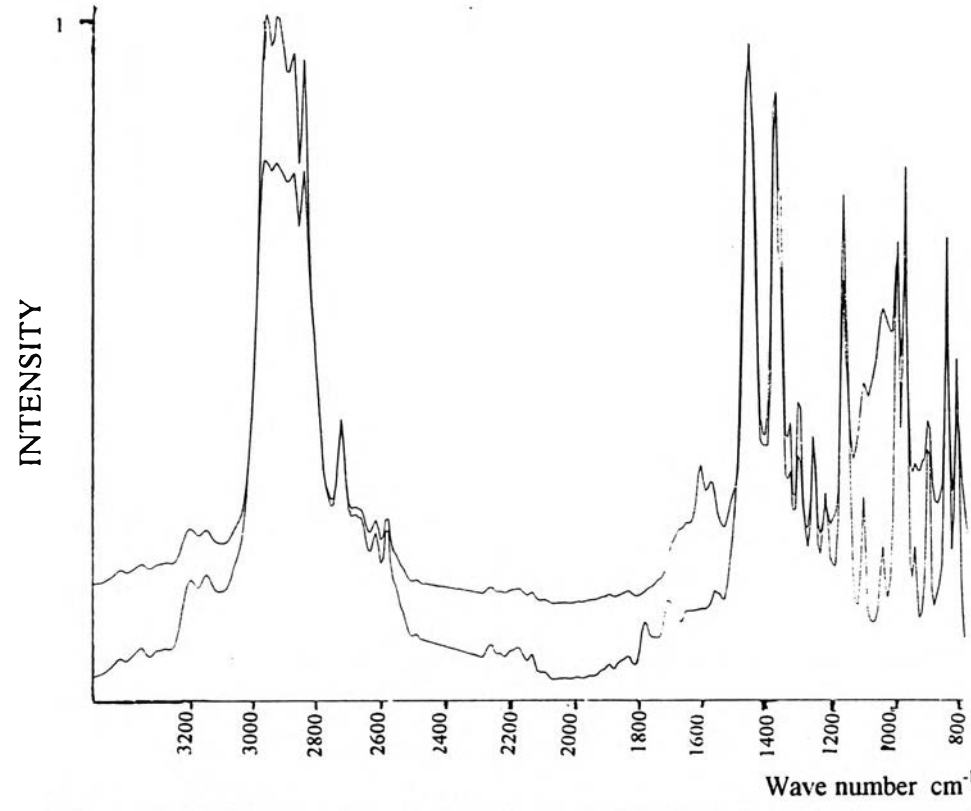

Figure 3.6 DRIFT spectra of MAPP and MAPP grafted with modified silicate clay.

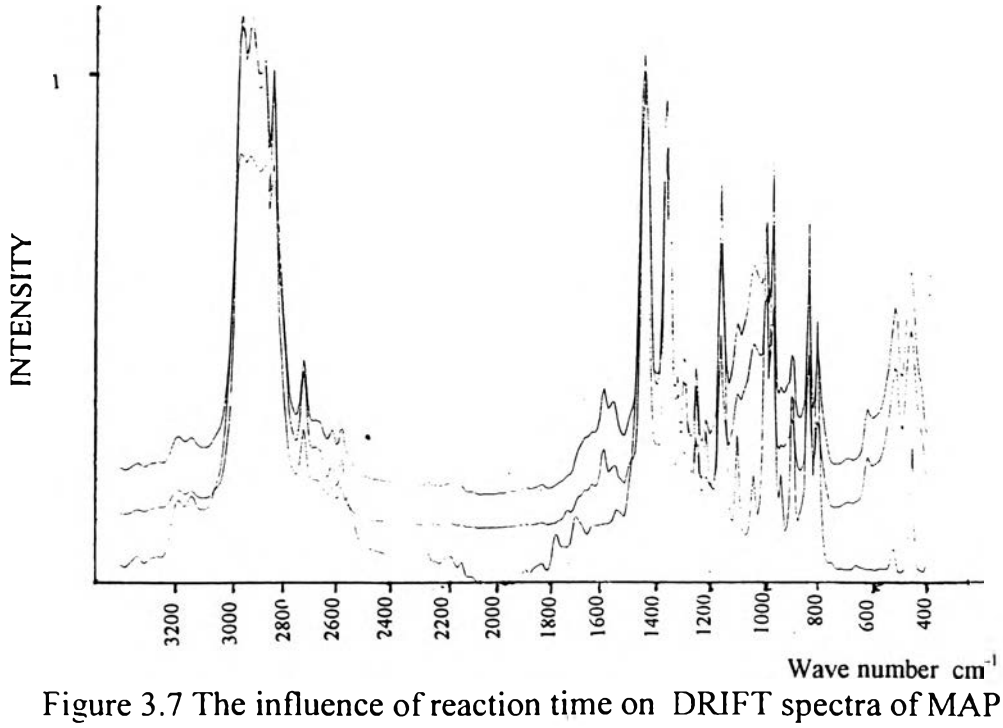

Figure 3.7 The influence of reaction time on DRIFT spectra of MAPP grafted with modified silicate clay.

3.2.2 XRD Result

The delamination of the montmorillonite clay in the nanofiller was confirmed by the X-ray powder diffraction (XRD). As shown by the powder patterns in fig. 3.8, the basal peak position indicates that interlayer distance of montmorillonite is 22 °A. This result illustrates that the interlayer expanded by the interpenetration of the polymer into the basal spacing of the modified silicate clay.

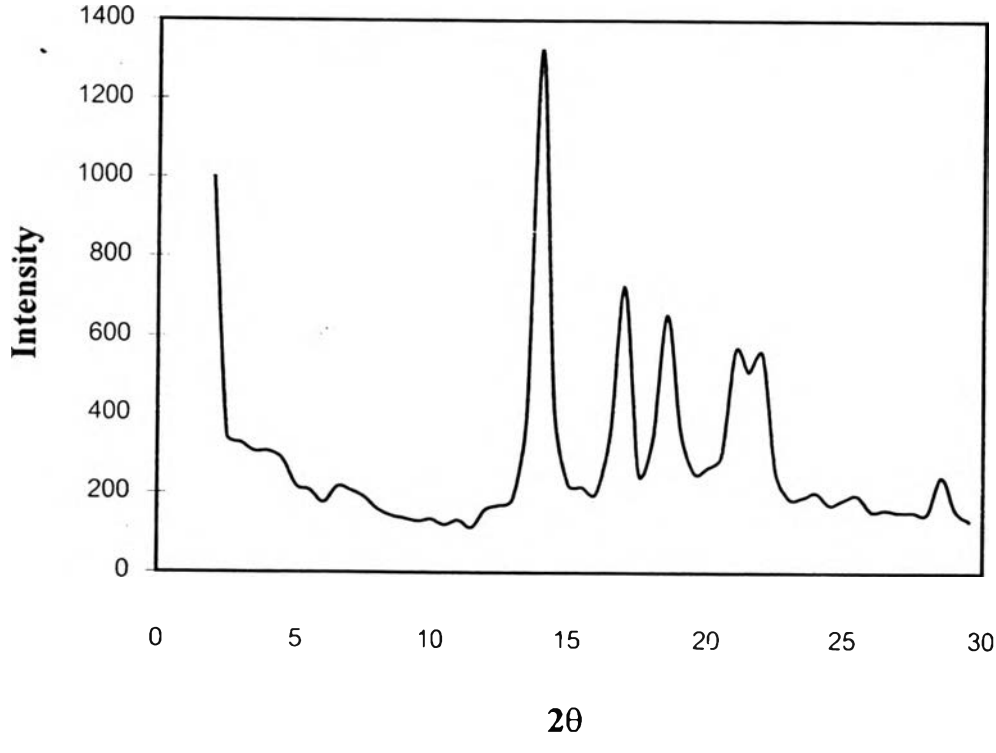

Figure 3.8 X-ray diffraction curves of MAPP and modified silicate clay.

3.2.3 TEM Result

A TEM micrograph of a section of 10 wt % modified silicate clay in MAPP is shown in fig. 3.9. The thick dark lines are intersection of silicate sheet of 10 °A thickness and the other region is the PP matrix. This photograph reveals that the micron - sized clay tactoids have been expanded by the polymer into accordian - like packets in which the interlayer spacings can range up to 22 °A. The majority of the particles are ~ 200 nm in thickness, consisting of approximately 6-7 silicate layers. In addition to these stacked layers some individually dispersed layer are observed. The irregular shape of the layer particles further indicates stacking and aggregation of individual layers.

Figure 3.9 TEM micrograph of 10% modified silicate clay in MAPP.

3.2.4 DSC Results

From DSC thermograms, the melting temperature (T_m) and heat of fusion were determined. The melting temperature indicates the density of the chain packing, while the area under the melting peak is the heat of fusion which can be converted to the percentage of crystallinity. We evaluated the heat of fusion using a value of 209 J/g for the 100 % crystalline polypropylene , and the calculations are shown in Appendix. Figure 3.10 shows the degree of crystallinity of the nanocomposite as a function of the filler content. The degree of crystallinity of the nanocomposite varies between 48 to 43.8 % independent of the amount of added filler content; these values are slightly lower than the value of pure PP of 50 %. This indicates that the fillers have a very weak nucleation effect leaving the crystalline structure of PP untouched. From these heat measurement, the melting temperature T_m was also obtained. The melting temperature was found to vary in the range of 169-167 ^oC as shown in fig. 3.11. Thus, it could be concluded that no change in the melting temperature on the addition of filler content was found

Karger [1995] found that the introduction of a second component - filler or reinforcement into the polymer can change its crystalline structure, which may affect properties. Some fillers have a very strong nucleating effect such as talc, while many other fillers have shown a weak nucleation effect and others make the crystalline structure of PP untouched. Varga [1995] classified talc as an active filler and $CaCO_3$, carbon black and dolomite as inactive ones.

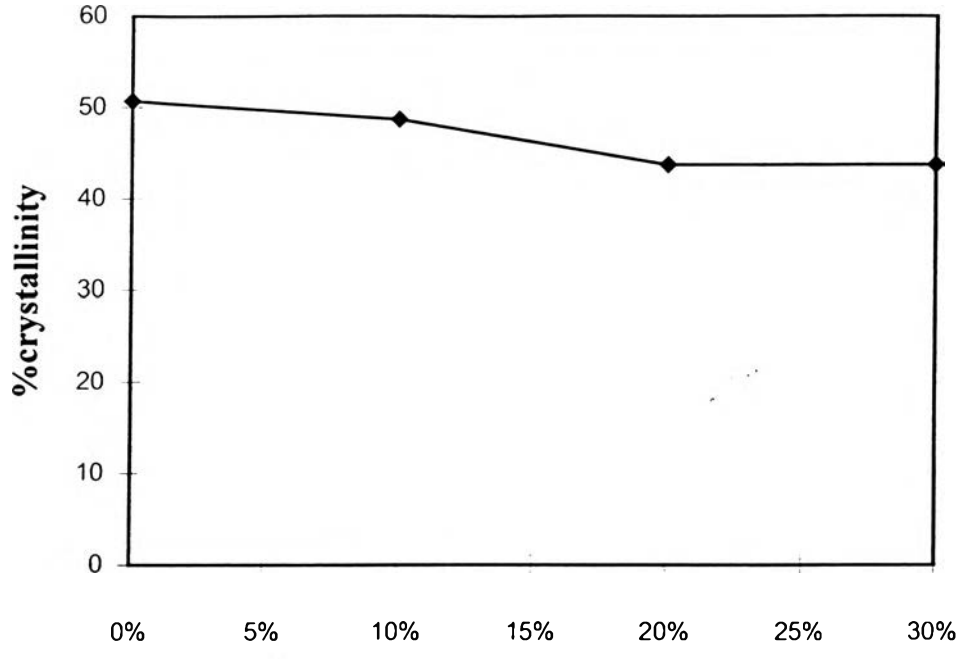

Figure 3.10 The degree of crystallinity of nanocomposite as the effect of filler content.

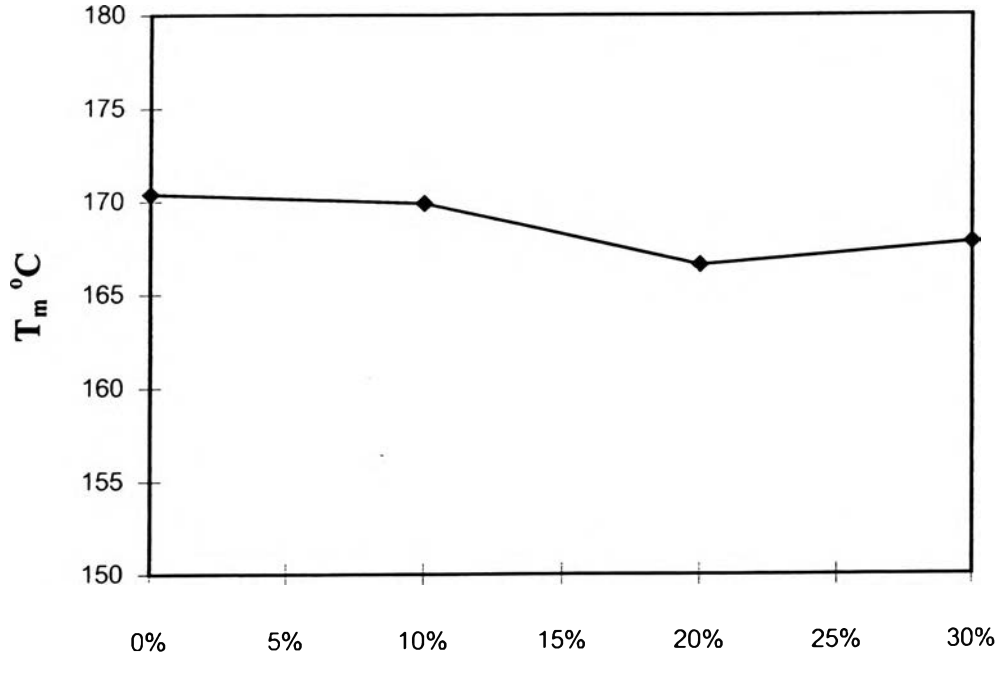

Figure 3.11 The melting temperature of nanocomposite as a function of filler content.

3.3 Mechanical Properties Testing

Three types of test were conducted: extension, flexural and impact tests. We are interested in investigating the effect of filler content, clay content and silane concentration.

Notation for the symbol in the graph is S/C/F; S is the weight % of silane concentration used in the silicate clay, C is the weight % clay content in the nanofiller, F is the weight % nanofiller content in the nanocomposite. For example, S/C/F: 2/X/10; means that this composite contains 10 wt % of nanofiller in the nanocomposite and the clay content is to be varied at the fixed amount of 2 wt % silane concentration used in the modification of silicate clay.

3.3.1 Effect of Filler Content

We tested two sets of nanocomposite as a function of filler content. One set is S/C/F: 2/10/X, another is S/C/F: 2/60/X.

Because the filler is finely dispersed, the modulus increases by several fold even for addition of only a few percent by weight. Figure 3.12a shows the tensile modulus of polypropylene nanocomposite as a function of filler content at fixed 10 and 60 wt % clay contents. There is a significant change in the tensile modulus when the small amount of filler content was added (1 - 5 %). At 0 % filler content, E = 2.0 GPa. For S/C/F: 2/10/X at 5 wt % filler content of nanocomposite E jumps to 16 GPa, an increase by a factor of 8. Beyond 5 wt % filler content E seems to reach an asymptotic value of about 18 GPa. For the other set of PP nanocomposite [S/C/F: 2/60/X] we see the similar behavior on the tensile modulus; at 5 wt % filler content E jumps to 18 GPa. It attains an asymptotic value of about 20 GPa for filler content greater than 5 wt %.

Significant increases on tensile strength require slightly higher degree of loading. Figure 3.12b shows the tensile strength as a function of filler content. There is a slight increase in the tensile strength between 1-5 wt. % filler content, for both sets of the samples [S/C/F: 2/10/X and S/C/F: 2/60/ X]. Above 5 wt % filler, there is a jump in σ_y for the set of S/C/F: 2/10/X from 33 MPa at 5 wt % filler to 42 MPa at 10 wt % filler. Beyond 10 wt % filler we obtaine an asymptotic value of σ_y at 53 MPa. For the set of sample S/C/F: 2/60/X, σ_y increases continuously with the filler content until reaching an asymptotic value of 68 MPa.

Chiang and Yang [1988] studied the properties of a composite made up of acrylic acid - grafted polypropylene and mica powder treated with a silane coupling agent. They found that the tensile strength and tensile modulus increased with an increase in mica content. The tensile modulus increased from 6.2 GPa to 13.4 GPa as the mica content increased from 0 to 60 phr. This work therfore, as an example of using silane grafting to improve mechanical perforemance.

Felix and Gatenholm [1991] investigated the nature of adhesion in composites of modified cellulose fibers and polypropylene-maleic anhydride copolymer. They found that the fiber treatment improved interfacial adhesion, yielding a stronger and more ductile material. At a fiber loading of 40 % the strength at yield increased by 80 %. In the case of 10 % fiber content, the corresponding value increased by 20 %.

Figure 3.13a shows the flexural modulus for samples of polypropylene and polypropylene nanocomposites. The flexural modulus increases continuously with the filler content until reaching asymptotic values of 1.6 GPa and 1.7 GPa for the sample sets of S/C/F: 2/10/X and 2/60/X respectively.

Figure 3.13b shows the dependence of flexural strength on the filler content. The flexural strength increases continuously with filler content. The flexural strength approaches a constant value of 60 MPa when the filler content is greater than 10 wt %. The flexural strength of S/C/F: 2/60/X nanocomposite at 30 wt % filler content is 1.5 times greater than that of pure PP. The increase in flexural strength is directly related to the increase in filler content as the load can be distributed due to the adherence of the filler surface. The most noticeable change in flexural strength is an increase (~50%) of the ultimate strength, presumably due to a change of fracture mechanism induced by the presence of mineral particles.

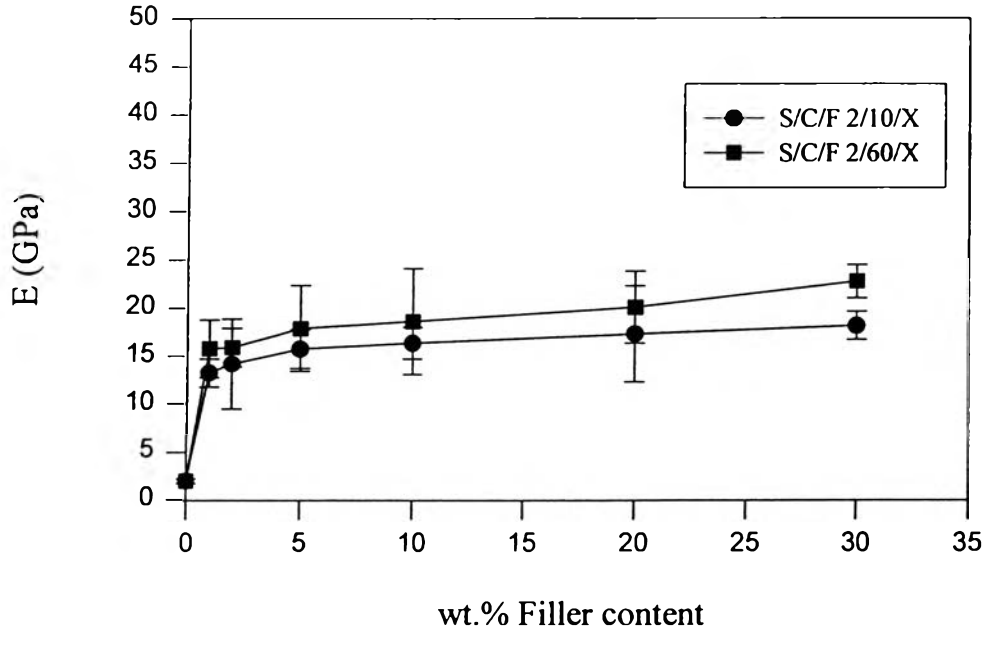

Figure 3.12 (a) The dependence of tensile modulus on filler content.

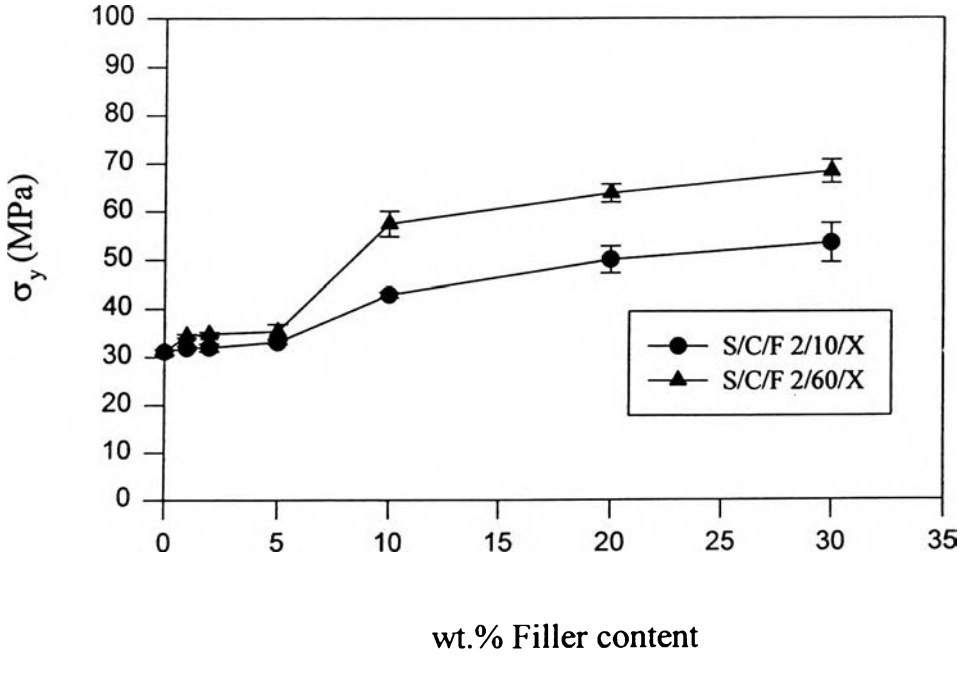

Figure 3.12 (b) The dependence of tensile strength on filler content.

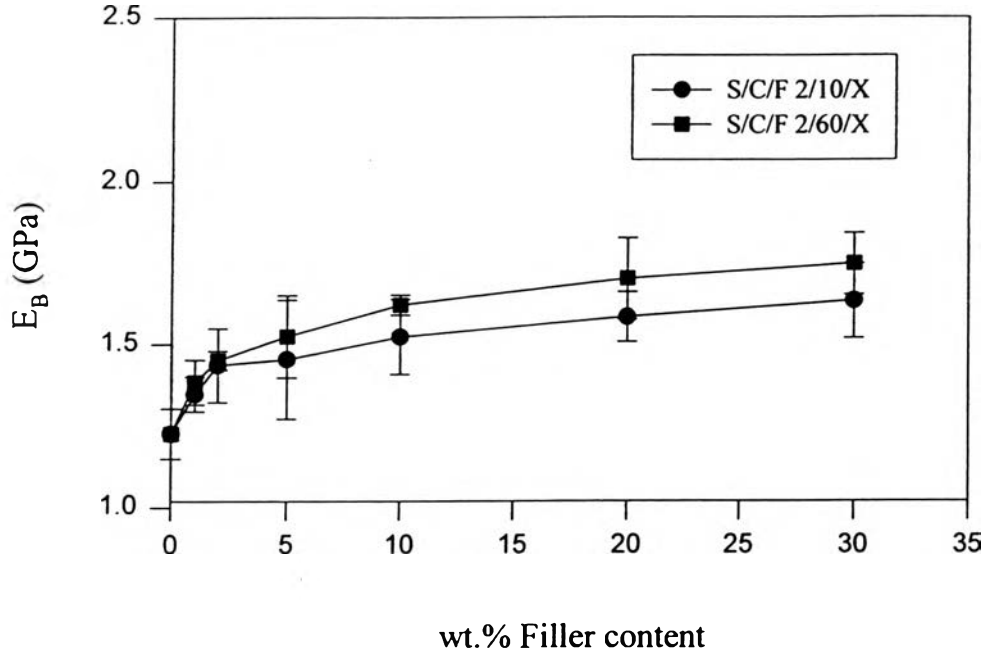

Figure 3.13 (a) The dependence of flexural modulus on filler content.

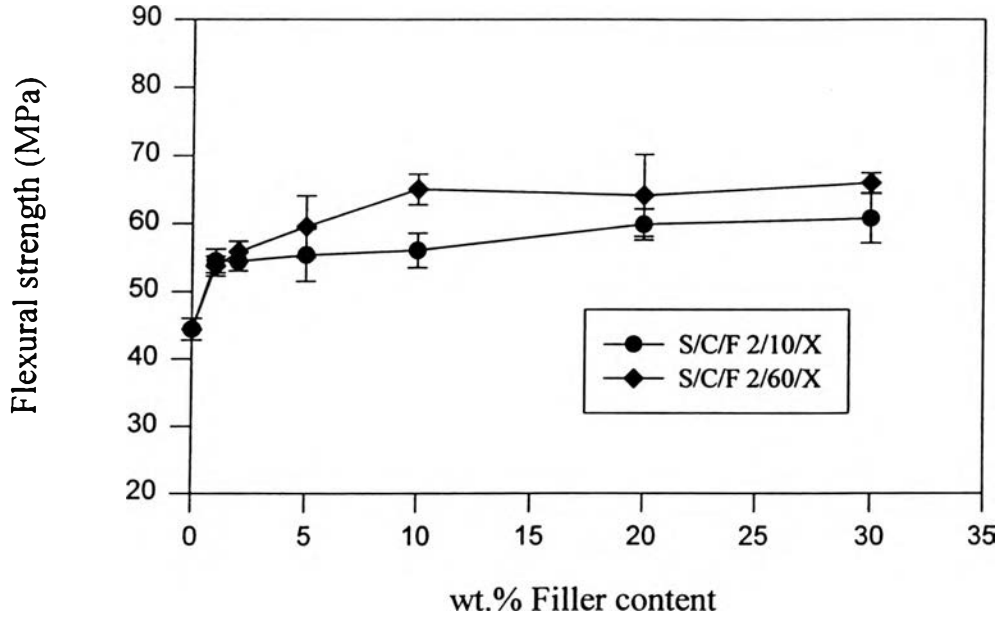

Figure 3.13 (b) The dependence of flexural strength on filler content.

The elastic and yield properties can be affected by the presence of fillers. This is a well known fact for semi-crystalline polymers in which the amorphous phase is in the rubbery state. The elastic modulus and yield stress depend strongly on the crystallinity ratio, which is globally almost constant for these sets of PP nanocomposites. However, it can undergo significant changes in the vicinity of mineral particles.

The positive effects on both tensile and flexural modulus and strength are presumably caused by the reinforcement effect which increases with anisotropy of the modified silicate particle, the particle interaction with the MAPP and the finely dispersion of the silicate particle in the matrix. We have found that the MAPP molecules were chemically bonded onto the filler surface through the use of silane coupling agent. Consequently, load can be transferred from the matrix to the filler particles inducing the increases in both tensile and flexural modulus and strength with the filler content. Comparing the two sets of tested polypropylene nanocomposites [S/C/F: 2/10/X and S/C/F: 2/60/X], the slightly higher value in the tensile and flexural properties can be obtained for 60 wt % clay content in nanofiller, this result is caused by the anisotropy of the clay particles, which has a strong effect on the tensile and flexural properties.

Figure 3.14 shows the impact resistance of S/C/F: 2/10/X and S/C/F: 2/60/X nanocomposite as a function of filler content. A gradual drop of the impact strength is observed at high filler concentrations. The fact that the impact strength of the composite is lower than that of unmodified PP is perhaps due to the addition of the nanofiller whose modified silicate clay still form a stack of layers. Under the effect of external load these clays induce stress concentrations, the stress distribution and local stress maximums developing in the composite can obviously influence its deformation and brittle resistance.

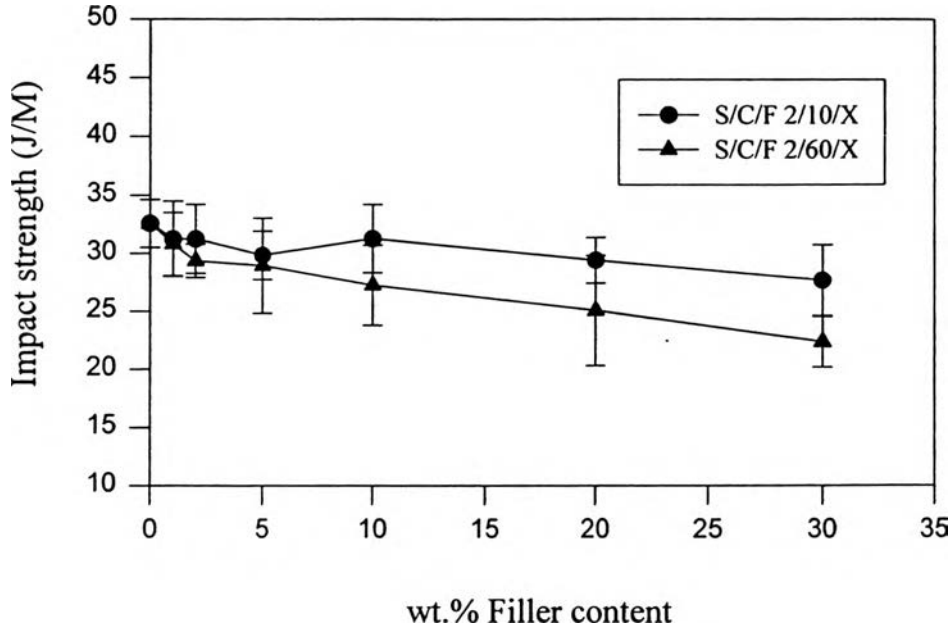

Figure 3.14 The dependence of impact strength on filler content.

3.3.2 Effect of Clay Content

We tested two sets of nanocomposites as a function of clay content. One set contained 10 wt % nanofiller in PP nanocomposite, another contained 30 wt % nanofiller in PP nanocomposite.

Figure 3.15a shows the tensile modulus of polypropylene nanocomposite as a function of clay content at fixed 10 and 30 wt % filler contents. There is a significant change in the tensile modulus when a small amount of clay content was added (1 - 5 wt %). At 0 wt % clay content E = 1.9 GPa, for S/C/F: 2/X/10 at 5 wt % clay content of nanocomposite E jumps to 15.5 GPa, an increase by a factor of 8. Beyond 5 wt % clay content E seems to reach an asymptotic value of about 18 GPa. For another set of PP

nanocomposite [S/C/F: 2/X/30] we can see the similar behavior on the tensile modulus, at 5 wt % clay content E jumps to 16 GPa. E reaches an asymptotic value of about 24 GPa for clay content greater than 5 wt %.

Figure 3.15b shows the tensile strength as a function of clay content. There is a slight increase in the tensile strength between 1-5 wt % clay content, for both set of sample [S/C/F: 2/X/10 and S/C/F: 2/X/30]. Above 5 wt % clay, there is a jump in the tensile strength for the set of S/C/F: 2/X/10 from 33 MPa at 5 wt % clay to 42 MPa at 10 wt % clay. Beyond 10 wt % clay we obtained an asymptotic value of the tensile strength = 60 MPa. For the set of sample S/C/F: 2/X/30, the tensile strength increases continuously with the filler content until reaching an asymptotic value of 75 MPa.

Our results agree with the work of Galeaki [1990]. He studied on polyolefins filled with chalk or calcium carbonate. The elastic modulus increase dramatically with an increase in content of the filler. At 60 wt % of calcium carbonate in linear polyethylene the young's modulus increased by a factors of 10 as compared to plain polyethylene.

Maiti and Mahapatro [1991] studied the mechanical properties of iPP/ $CaCO_3$ composites with and without a titanate coupling agent. They found that the modulus of untreated $CaCO_3$ - filled composites showed a steady increase with filler concentration, reaching a maximum at 35.4 wt % filler content, the value of the tensile modulus was almost double that of iPP. But for the filler with surface treatment by the coupling agent, they found a doubling of E for iPP at only 4 volume % filler, beyond this volume content the increase was only marginal.

Figure 3.16a shows the flexural modulus of polypropylene nanocomposite as a function of clay content at fixed 10 and 30 wt % filler contents. There is a change in E_B when a small amount of clay content is added (1 - 5 wt %). At 0 wt % clay content, E_B = 1.226 GPa, for S/C/F: 2/

X/10 at 5 wt % clay content of nanocomposite, E_B jumps to 1.489 GPa, about 20 wt % increase. Beyond 5 wt % clay content, E_B reaches an asymptotic value of about 1.6 Gpa. For another set of PP nanocomposite [S/C/F: 2/X/30] also show the similar behavior for the flexural modulus. At 5 wt % clay content E jumps to 1.483 Gpa, until reaching an asymptotic value for clay content greater than 5 wt %.

Figure 3.16b shows the flexural strength as a function of clay content. There is a slight increase in the flexural strength between 1-5 wt % clay content, for both set of sample [S/C/F: 2/X/10 and S/C/F: 2/X/30]. Above 5 wt % clay content, there is a slight increase in flexural strength for the set of S/C/F: 2/X/10 from 56.23 MPa at 5 wt % tensile to 59.64 MPa at 60 wt % clay. For the set of sample S/C/F: 2/X/30, the flexural strength increase continuously with the filler content until reaching an asymptotic value of 64 MPa.

The restriction in polymer molecular diffusion in the polypropylene nanocomposite system in the presence of solid particles is due to an effective attraction potential between segments of the chain sequential to the repulsive potential that the polymer is subjected to when it approaches the silicate particles. The tensile and flexural modulus and strength are increased with the increase in clay content in both sets of PP nanocomposite [S/C/F: 2/X10 and S/C/F: 2/X/30]. There are three factors which influence these properties: (1) the MAPP content which give the physical entanglement effect with PP, (2) ionic bonding between MAPP and silicate clay through the siloxane bond, (3) the anisotropy of the silicate particle, which the greatest advantage of the anisometric fillers is the possibility of transferring the load. When the clay content is low, factors 1 and 2 contribute more toward these properties. When the clay content is large, factor 3 is more influential

than the other factors. So the rise in these properties at low volume fraction is higher than those of high volume of clay, this is due to the higher adhesion of silicate particle and MAPP at low concentration of clay content.

If we compare two sets of PP nanocomposite 10 wt % and 30 wt % filler content, we found that 30 wt % filler content [S/C/F : 2/ X/30] gives higher value of both modulus and strength when compared with the set of S/C/F : 2/X/10. This may be due to two effects: the reinforcement effect of filler and the physical entanglements effect of MAPP with PP.

Figure 3.17 shows the variation of impact strength of S/C/F : 2/X/10 and S/C/F: 2/X/30 polypropylene nanocomposites as a function of clay content. A dramatic drop of the impact strength is observed at high clay concentrations. For the set of S/C/F :2/X/10 at 60 wt % clay content the impact strength decreases to a value of 24.32 J/m compared with 32.57 J/m of the pure PP. For S/C/F : 2/X/30 the value of impact strength is 22.34 J/m. The reduction in impact strength with increasing volume fraction of clay content is possibly caused by the increase in stress concentrations around the clay particles.

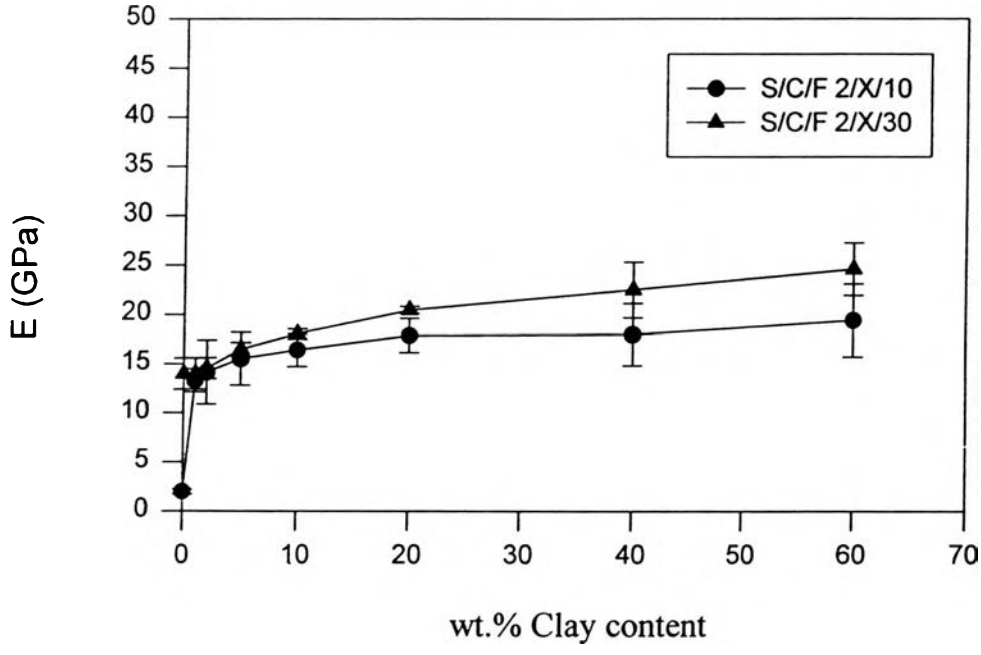

Figure 3.15 (a) The dependence of tensile modulus on clay content.

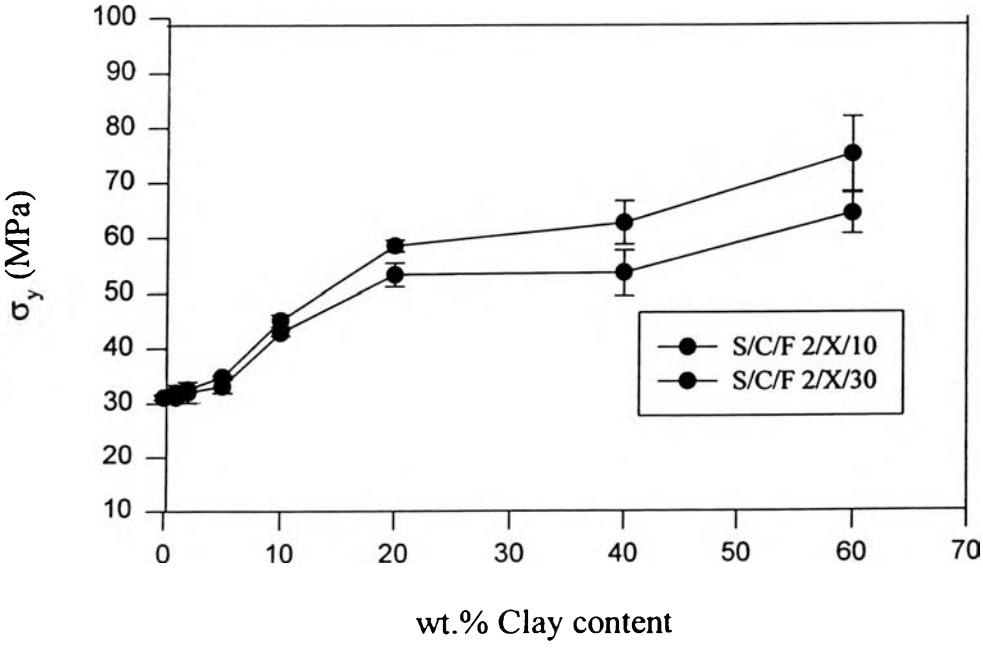

Figure 3.15 (b) The dependence of tensile strength on clay content.

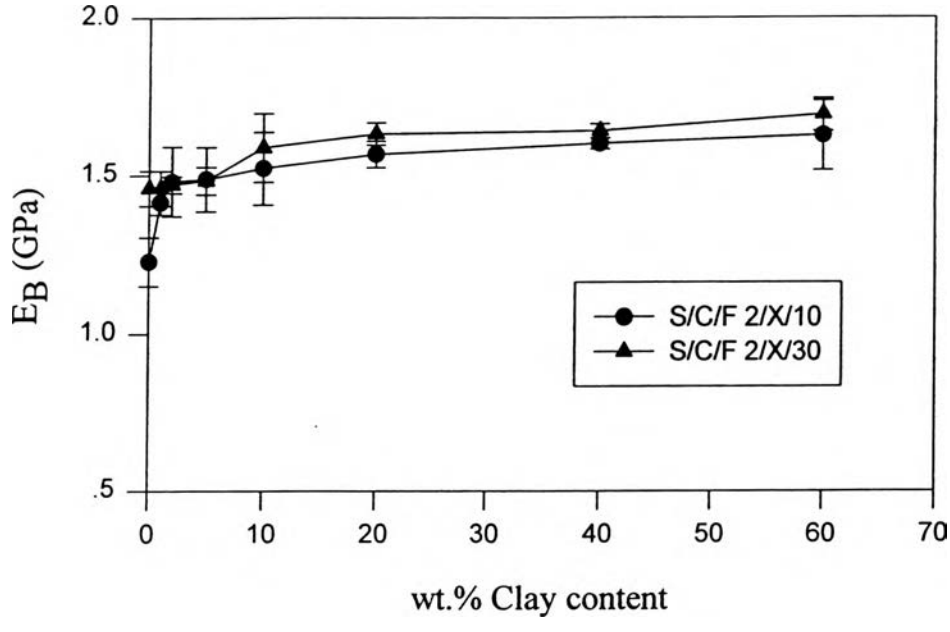

Figure 3.16 (a) The dependence of flexural modulus on clay content.

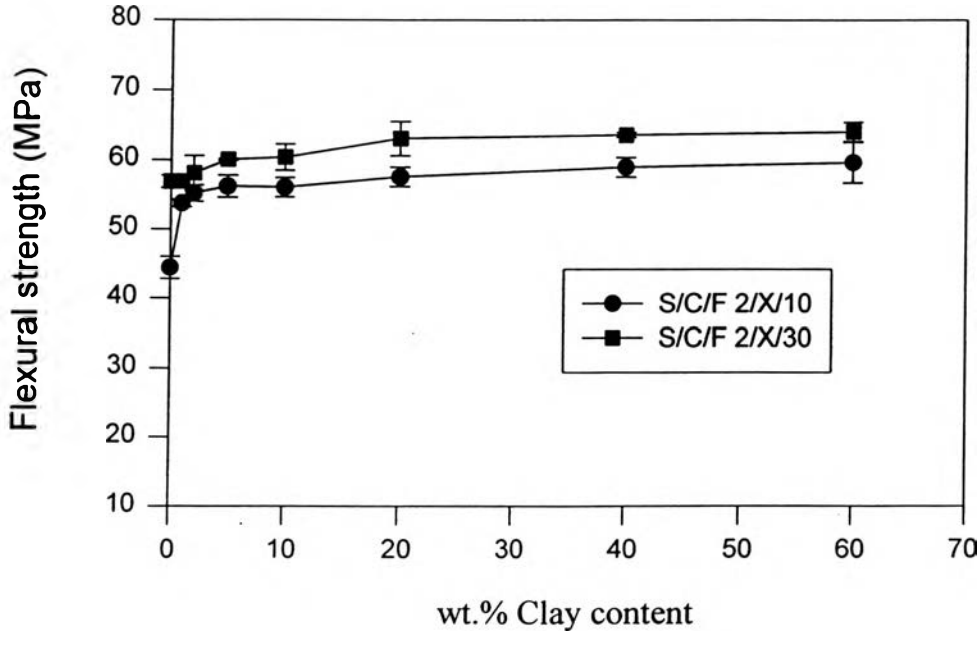

Figure 3.16 (b) The dependence of flexural strength on clay content.

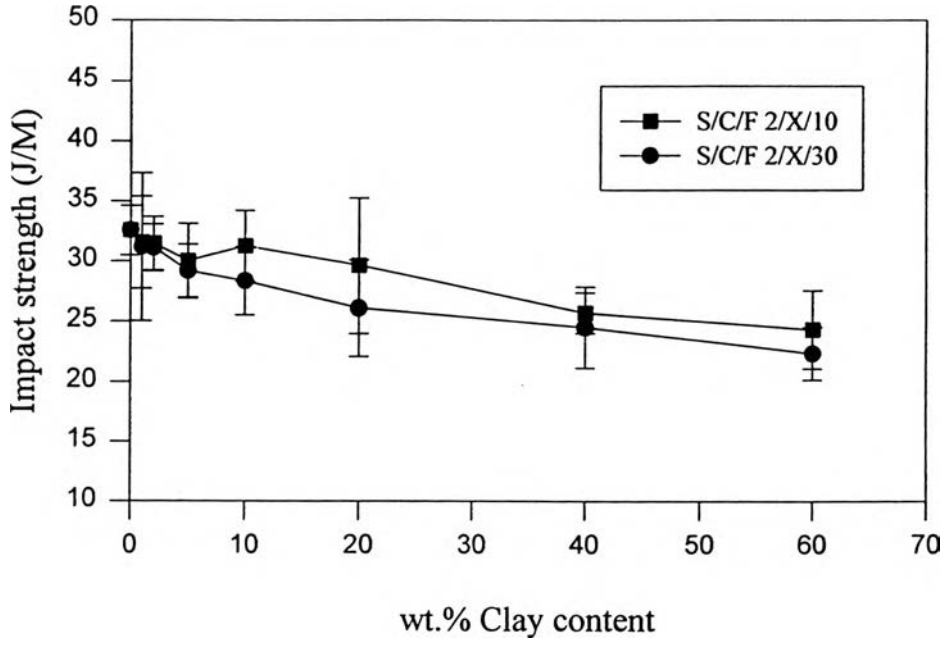

Figure 3.17 The dependence of impact strength on clay content.

3.3.3 Effect of Silane Concentration

We investigated two sets of polypropylene nanocomposites as a function of silane concentrations (0-30 wt %). One set of samples contained 10 wt % clay content in 10 wt % nanofiller, another set of samples contained 60 wt % clay content in 10 wt % nanofiller.

Figure 3.18a shows the tensile modulus of polypropylene nanocomposites as a function of silane concentration at the fixed 10 and 60 wt % clay content in nanofiller. There is a dramatic increase from 11.5 to 18 GPa of the tensile modulus when the surface of the clay was treated with 2-5 wt % silane concentrations. When the amount of the silane is greater than 5 wt %, there is a drop in the tensile modulus to an asymptotic value of 12 GPa. For S/C/F: X/10/10 at 5 wt % silane concentration, E drops to an asymptotic value

of about 12 GPa. For another set of PP nanocomposites [S/C/F: X/60/10] also showed a similar behavior on the tensile modulus, at 5 wt % silane concentration E jumps to 18 Gpa; then drops to an asymptotic value of 14 GPa.

The tensile strength property of PP nanocomposites is shown in fig. 3.19b. For both sets of PP nanocomposite [S/C/F: X/10/10 and S/C/F: X/60/10], the tensile strength increases slightly with the effect of clay content as can be seen only when silane concentration is above 10 wt %.

Figure 3.19a shows the flexural modulus of polypropylene nanocomposite as a function of silane concentration at the fixed 10 and 60 wt % clay content in nanofiller. There is a jump from 1.3 to 1.6 GPa when the surface of the clay was treated with 2-5 wt % silane concentration. When the amount of the silane is greater than 5 wt %, there is the drop in the flexural modulus to an asymptotic value of 1.3 GPa. For S/C/F: X/10/10 at 5 wt % silane concentration E drops to an asymptotic value of about 12 GPa. Another set of sample of PP nanocomposites [S/C/F: X/60/10] shows the similar behavior on the flexural modulus, at 5 wt % silane concentration E_B jumps to 1.634 GPa, then drops to an asymptotic value of 1.3 GPa.

The flexural strength property of PP nanocomposites is shown in Figure 3.19b. For both sets of PP nanocomposite [S/C/F: X/10/10 and S/C/F: X/60/10], the flexural strength increases slightly with the effect of clay content which can be seen only when silane concentration is about 0-10 wt %.

Our results are consistent with the work of Trotignon et al.[1986] who found a strong increase and a maximum in the strength of PP-mica composites as a function of the silane used. At 1.5 wt % silane concentration, the composite had the maximun value of the tensile strength (~ 40 MPa) beyond this the tensile strength decreased.

Graf et al. [1995] investigated the interphase structure by use of DRIFT and its consequent mechanical properties of γ-MPS /bisphenol-A-fumarate polyester resin composite as a function of the amount of γ-MPS. They founded that the flexural strength increased largely within the low amount of γ-MPS, indicating only chemisorbed silane are effective and there was a maximum in the flexural strength and modulus at low amount of silane.

In the PP nanocomposite system, MAPP had grafted onto the silane coupling agent at the silicate surface. There are some optimal amount of silane that should be used [2-5 wt %]. The formation of a bond between the silanol groups of the hydrolysed coupling agent on the silicate surface formed multilayers on the surface of the silicate filler, the first layer is chemically bonded to the surface, and the outer layer is physisorbed silane.

At 2-5 wt % silane concentration, the coverage of the filler surface polymer layer is capable of interdiffusion with the matrix and forming the chemisorbed layer to the surface. So these factors affect both the stress transfer and formation diffusing interphase with acceptable deformability. These give rise to the high modulus and strength. Beyond 5 wt % silane concentration, there are the reductions of both tensile and flexural moduli as a result of the diffusion of physisorbed silane into resin.

Figure 3.20 is the plot of the impact strength of polypropylene nanocomposites versus the silane concentrations. The coupling agent increases the impact strength relative to the untreated nanocomposite at 0 wt % silane concentration used. The maximum of the absorbed energy is found between 2-5 wt % of silane concentration and then it decreases. The effect of clay content is noticeable at high silane concentration.

This improvement of impact properties with coupling agent treatment could be due to several possible effects: (1) morphological differences in the composite due to the surface treatment. Both the silane and

the polymer can interdiffuse into each other and then crosslink, making some changes in the morphological structure. (2) surface tension energy differences due to the silane treatments at the surface. There is a decrease in particle - particle friction due to coupling agent treatment. (3) a plasticizing effect due to the presence of a coupling agent, which can make the system more ductile due to the load transfer across the interface.

Our results are consistent with the work of Scott et al. [1987]. He studied the effects of the use of coupling agents on PE/ filler composite on the impact strength. For gamma-methacryloxypropyltrimethoxysilane, they found that the use of one equivalent monolayer improved the impact strength relative to the use of five equivalent monolayers. They noted that there is probably some optimal silane amount for the surface treatment.

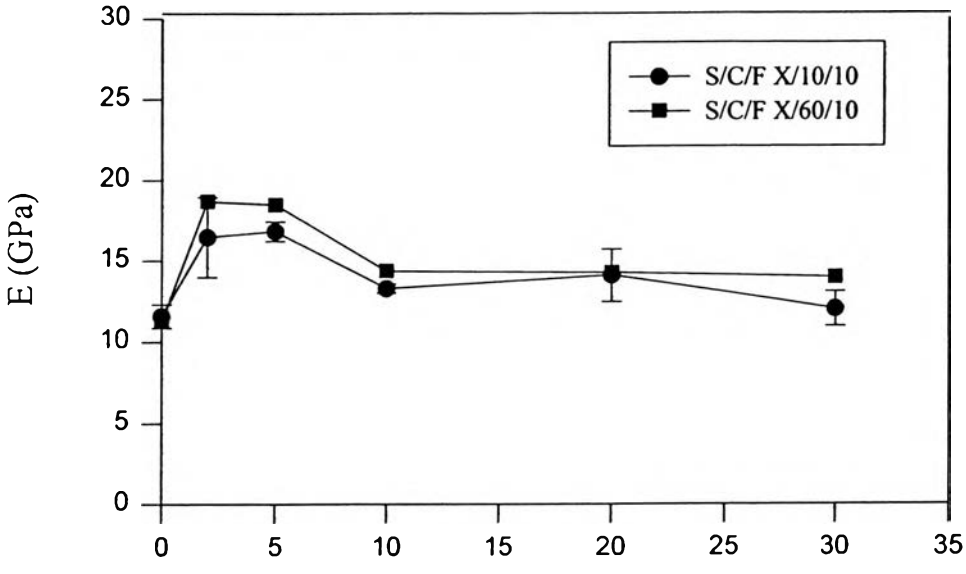

Figure 3.18 (a) The dependence of tensile modulus on silane concentration.

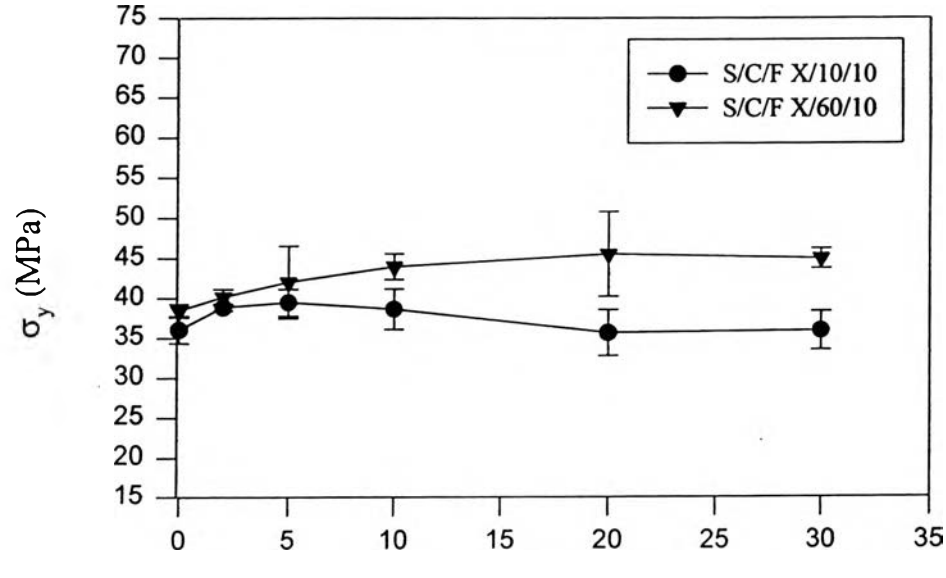

Figure 3.18 (b) The dependence of tensile strength on silane concentration.

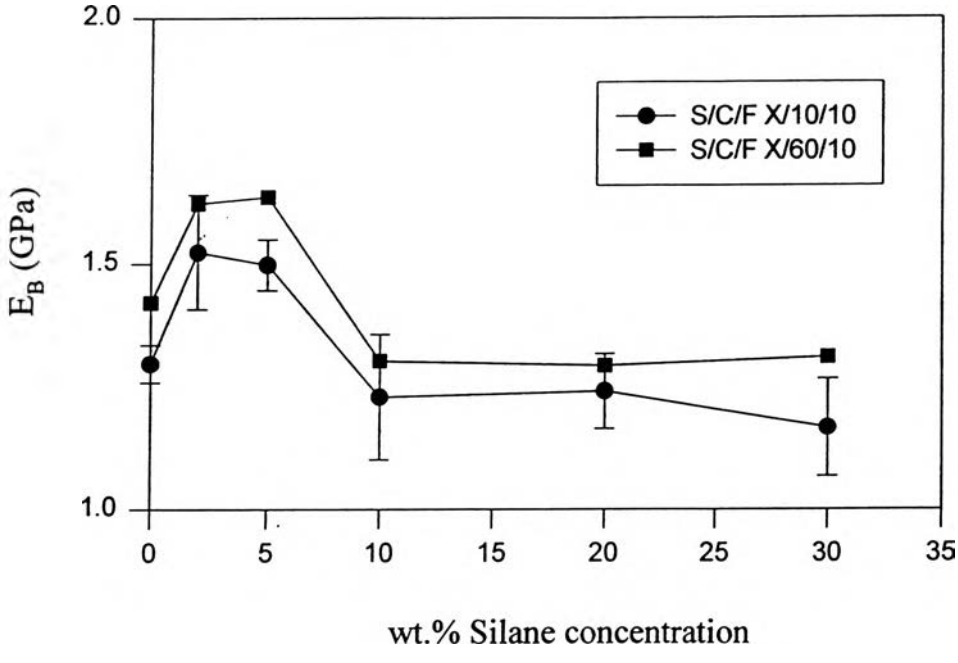

Figure 3.19 (a) The dependence of flexural modulus on silane concentration.

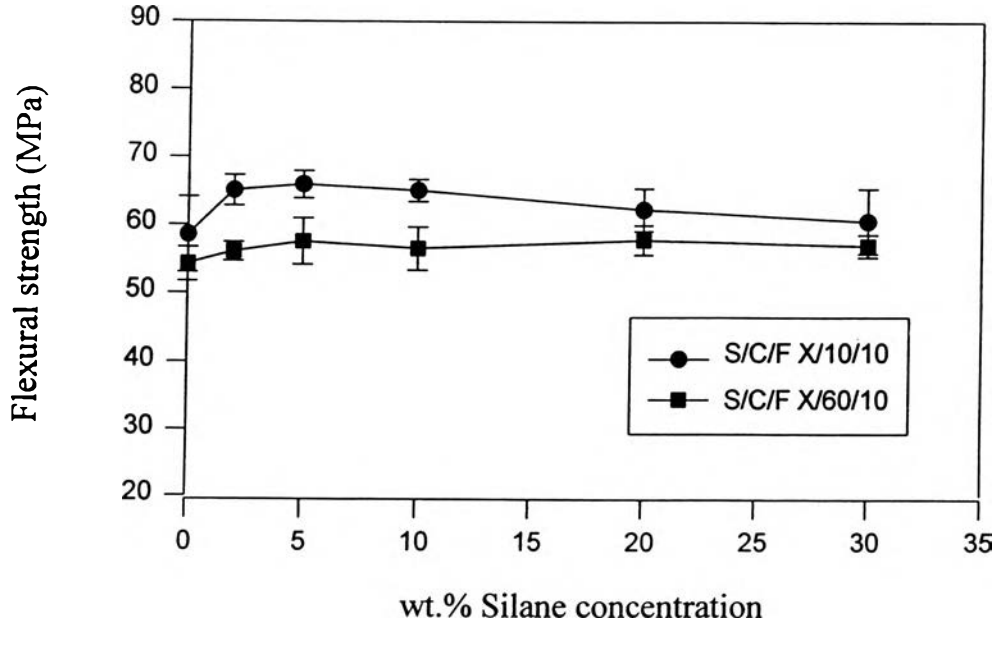

Figure 3.19 (b) The dependence of flexural strength on silane concentration.

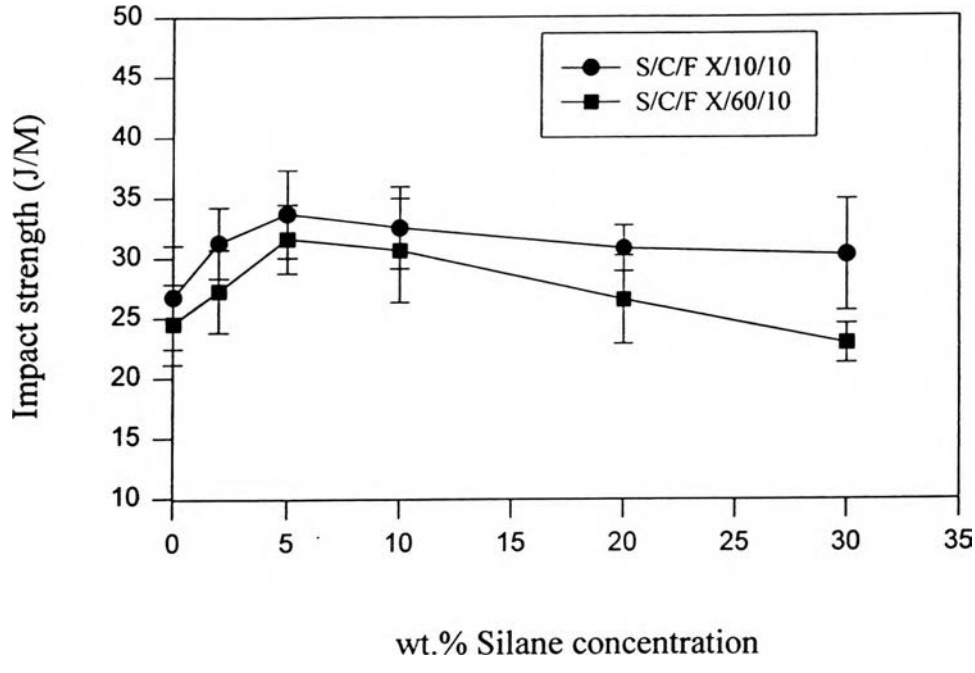

Figure 3.20 The dependence of impact strength on silane concentration.

3.3.4 Slow Crack Growth (SCG) Testing

The crack growth behavior of pure PP and the polypropylene nanocomposites are shown in fig. 3.21 where crack opening displacement is plotted against time. The crack opening displacement (COD) was measured by the zoom stereomicroscope with the magnification of 13.7 at the room temperature of 24 ^{o}C. The crack opening displacement (COD) corresponds to the length of the stress whitening beyond the notch tip. For each measurement, the sample was taken off the slow crack growth apparatus. The duration of measurement where the sample was under no loading was a mere fraction of 0.69 % of the total experimental time. Therefore, the off loading time was negligible in our experiment.

From this figure, we can divide the slow crack growth process into two regimes. The first regime encompasses the linear portion of the COD vs. time curve. The second regime corresponds to the time during which COD varies nonlinearly with time. At the end of the linear regime, we can define the time to initiate fracture as the time scale before a fast crack starts [Zhou and Brown (17, 1994)]. In fig. 3.21, we find that the time to initiate fracture is 4320 min for the pure PP sample. This time increases to 7200 min when the nanocomposite sample contained 30 wt % filler content. We found that a substantial increase in the time to initiate fracture can be obtained when the nanocomposite contained only 10 wt % filler content; the time scale is possibly greater than 30,000 min. It should be noted that for this nanocomposite, two measurement runs were carried out and that the average COD was taken. At a particular experiment time, an average COD may be slightly lower than an average COD at a shorter experimental time.

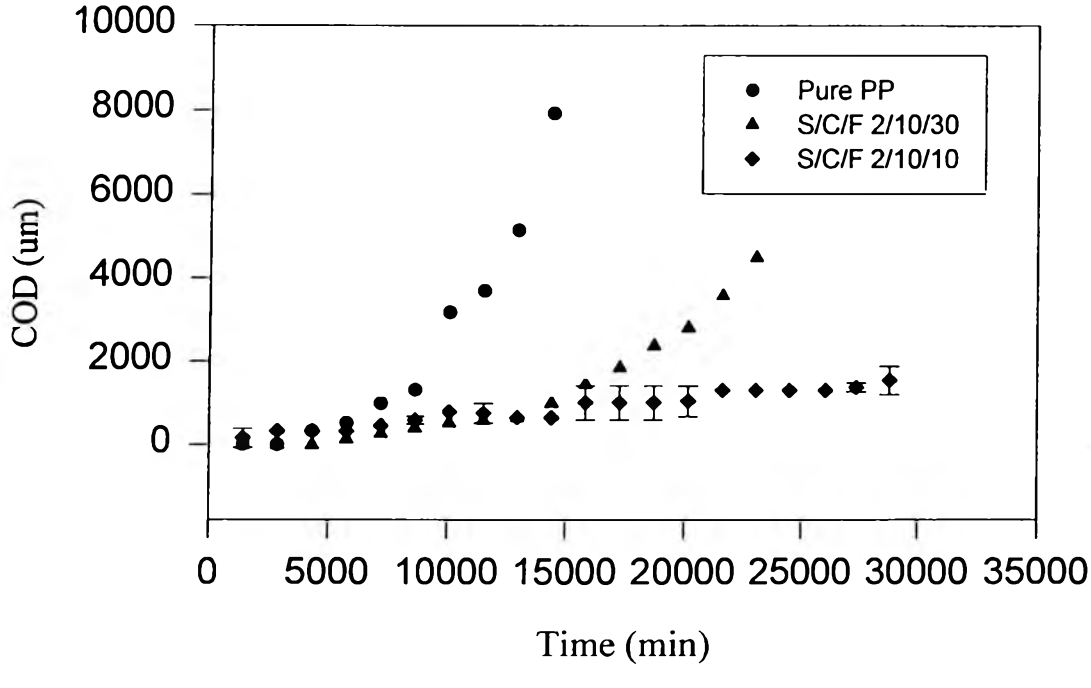

Figure 3.21 The slow crack growth behavior of modified polypropylene.

In regime I or the initial linear part of the COD curves, entanglements between tie chains and the matrix of crystalline PP are dominant factors which control the slow crack growth behavior. Disentanglements occur slowly but continuously. In regime II, the slope of the curves begins to grow with time. Here we expect that more severe disentanglements and chain scissions of the tie molecules have started leading to a faster pace of crack opening.

The resistance to SCG is based on a simple model [Brown, 1991]. Tie molecules and the crystals forms a network within the fibrils of the craze. When a stress is applied to this structure, a force is transmitted to tie molecules. The time to complete failure is determined by the rate of disentanglement of the tie molecules, which varies directly with the force exerted by the tie molecule. Fracture occurs when the tie molecules are torn apart and the rate of SCG increases. When PP was modified by the nanofiller, for clay of small particle size and with good level of filler dispersion, extra physical linking occurs between crystalline structures. The tie molecules function as a linkage device. For the nanocomposite of 30 wt % modified filler content , it has a better resistance to SCG than the pure PP. But for the nanocomposite of 10 wt % modified filler content, the resistance to the SCG is found to be optimal. This is probably a result of a finer degree of filler delamination.